

Supporting information

Cruciform Shape Hole Shuttle Materials Based on Spiro [Fluorene-9, 9'- Xanthene] for Defect Passivation in Perovskite Solar Cells

Bommaramoni Yadagiri,^a Sanjay Sandhu,^a Ashok Kumar Kaliamurthy,^a Francis Kwaku Asiam,^a
Jongdeok Park,^a Appiagyei Ewusi Mensah,^a and Jae-Joon Lee^{a*}

^aDepartment of Energy Materials and Engineering, Research Center for Photon energy Harvesting
& Conversion Technology (*phct*), Dongguk University, Seoul, South Korea.

Corresponding author email: jjlee@dongguk.edu

1. Experimental Section

1.1 Materials

Catechol, 2,7-dibromofluorenone, benzo[b]thiophene-2-boronic acid, and [4-[Bis(4-methoxyphenyl) amino] phenyl] boronic acid was obtained from commercially available sources. The reaction and purification solvents, reagents and catalysts were purchased from commercial suppliers, which are used without further purification. All the chemical reactions were performed under the nitrogen atmosphere condition.

1.2 Measurement

The target compounds and intermediates were characterized by using ^1H - and ^{13}C - NMR spectra, which are measured in deuterated chloroform (CDCl_3) on a Bruker 500-MHz spectrometer. Tetramethylsilane (TMS) solvent was used as standard and peak multiplicity was reported as follows: s, singlet; d, doublet; t, triplet; m, multiplet; dd, doublet of doublet. The column chromatography was performed to purify intermediates and target compounds by using silica gel (100-200 mesh). The UV-visible absorption spectra in solution and solid film states were measured on Scinco S-3100 spectrophotometer. The electrochemistry measurements such as cyclic voltammetry (CV) and differential pulse voltammetry (DPV) were recorded with a CH Instruments with a scan rate of 100 mV/s in dichloromethane (DCM). Tetrabutylammonium hexafluorophosphate (TBAPF_6) (0.1M) was selected as the supporting electrolyte, with electrode systems such as the reference electrode (Ag/AgCl), the working electrode (carbon-glass), the counter electrode (Pt wire) and ferrocene/ferrocenium (Fc/Fc^+) as an external reference.

2. Perovskite fabrication process

2.1. Materials

All the compounds were directly used for the fabrication process without any additional modification until mentioned. Lead (II) iodide (PbI_2 , 99.999%), bis(trifluoromethane) sulfonimide lithium salt (Li-TFSI), and tris(2-(1H-pyrazol-1-yl)-4-tert-butylpyridine) cobalt (III) tris (bis (trifluoromethyl sulfonyl) imide) (FK209) were purchased from Tokyo Chemical Industry (TCI) Co., Ltd. (Japan). Methylammonium iodide (MAI, 99.99%) was acquired from Dyesol (Australia) and Tin (IV) oxide (SnO_2) (15% in H_2O) was purchased from Alfa Aesar. The organic solvents such as dimethyl sulfoxide (DMSO), dimethylformamide (DMF), acetonitrile (ACN), toluene, isopropanol (IPA), chlorobenzene (CB), 4-tert-butylpyridine (tBP) were purchased from Sigma-Aldrich. The Spiro-OMeTAD (2,2',7,7'-tetrakis-(N, N-di-p-methoxyphenylamine)-9,9'-spirobifluorene) was obtained from Lumtec (Taiwan). The FTO (fluorine-doped tin oxide) glass substrates were purchased from TEC 8, Pilkington.

2.2. Fabrication process of MAPbI_3 solar cells

The FTO substrates were sequentially cleaned with soap solution, distilled water, ethanol (EtOH), and IPA by sonication for 20 min each. These substrates were cleansed with N_2 gas and dried at 70 °C for 4 h. The FTO substrates were placed under the ultraviolet-ozone (UV- O_3) atmosphere for 20 min before electron transport layer (ETL) deposition. The ETL solution was prepared by diluting SnO_2 in 2-propanol and deionized water with volume/volume ratio of 1:3:3 v/v respectively. Then ETL was formed by spin coating the prepared solution at 4000 rpm for 30 s followed by annealing on hot plate at 100 °C and 180 °C for 10 min and 30 min respectively. The 1M MAPbI_3 precursor solution was prepared from PbI_2 and MAI materials and dissolved in

1:4 ratio of DMSO and DMF. The solutions of **SPX-TPA** (1 mg, 3 mg and 5 mg) and **SPX-BT** (1 mg and 3 mg) were prepared in 1 mL of chlorobenzene solvent. Next, the perovskite films were prepared by spin coating in two step-programs (1000 rpm for 10 s, 4500 rpm for 40 s) with 500 μ L of toluene (antisolvent) dropped on the substrate 10 s before the second step ends and resultant films were annealed at 100 °C for 30 min. After that, various amounts of **SPX-TPA** and **SPX-BT** were spin coated at 3000 rpm for 30 s without any post treatment. Next, the spiro-OMeTAD (73 mg/mL in chlorobenzene), with dopants tBP (28 μ L), Li-TFSI (28 μ L; 530 mg/mL in acetonitrile), and FK209 (18 μ L; 300 mg/mL in acetonitrile) was coated at 3000 rpm for 30 s. Finally, Au (80 nm) electrode was thermally evaporated under high vacuum level using a shadow mask to obtain Glass/FTO/SnO₂/MAPbI₃/**SPX-TPA** or **SPX-BT**/Spiro-OMeTAD/Au structured PSCs device (active area of 0.22 cm²).

2.3. Film and device characterizations

The UV–visible absorption spectra of perovskite films were measured by using Scinco S-3100 spectrophotometry. The morphologies of thin films were obtained by field emission scanning electron microscope (FESEM, JSM-6700F, JEOL). X-ray diffraction (XRD) studies were measured using an X-ray diffractometer (Rigaku D/Max-2500) with Cu-K α X-rays. The PV performance of fabricated cells was measured under 1 Sun illumination by a LAB50 solar simulator (McScience) attached with a Keithley 2400 source meter. The incident power of solar simulator was calibrated by a standard mono-Si solar cell (PVM-396, PV Measurements, Inc.) certified by the National Renewable Energy Laboratory (NREL). The external quantum efficiency (EQE) measurement was obtained by using a photo-modulation spectroscopy setup having a monochromatic xenon light source (McScience, K3100 Spectral IPCE Measurement System) and it was calibrated using a Si-photodiode certified from the National Institute for Standards and

Technology (NIST). X-ray photoelectron spectroscopy (XPS) measurement was conducted using a ULVAC-PHI Veresprobe II with Monochromatic Al K α energy source at ultra-high vacuum (10^{-9} Torr). The photoluminescence (PL) and time resolved PL (TRPL) measurements were performed by using fluorescence lifetime spectrometer (Quantaaurus Tau C11367-12, HAMAMATSU) with excitation by 464 nm laser (PLP-10, HAMAMATSU) pulsed at a frequency of 10 MHz. The Fourier Transform Infrared Spectroscopy (FTIR) was obtained by infrared spectrometer (Nicolet 6700 / Nicolet iS50, Thermo Scientific, USA).

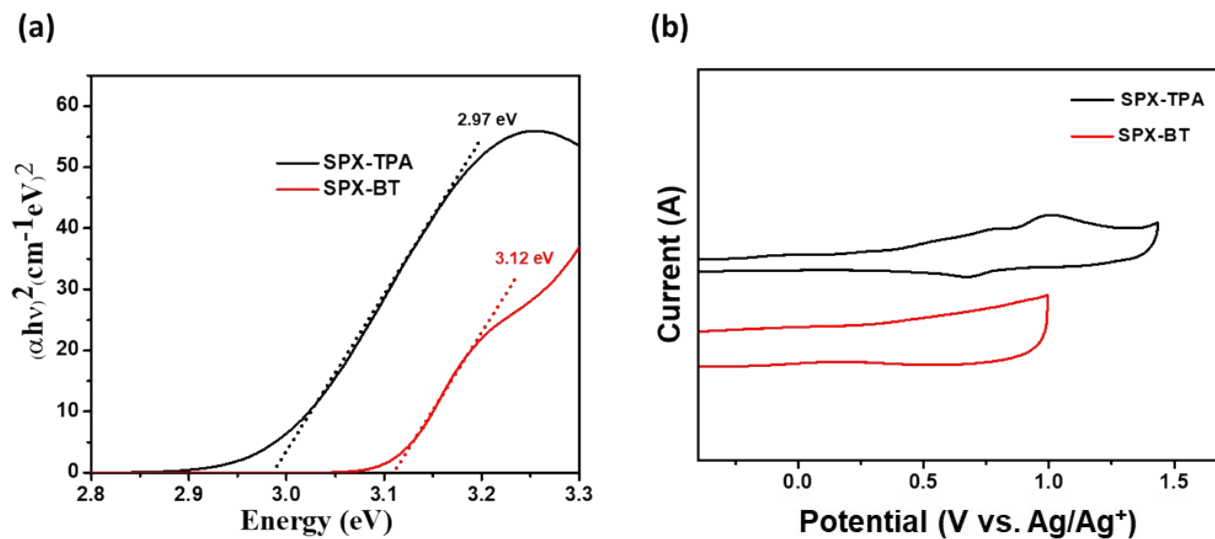
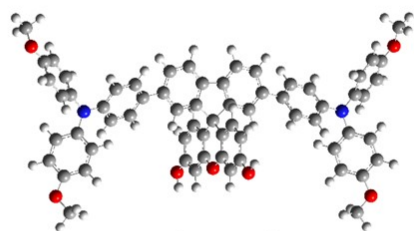


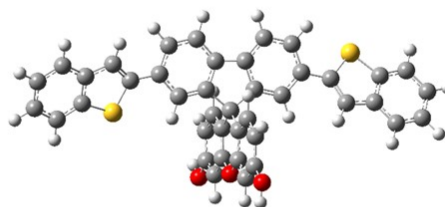
Fig. S1 (a) Tauc plots of **SPX-TPA** and **SPX-BT** from UV-visible absorption spectra performed in CHCl_3 solution. (b) Cyclic voltammetry (CV) of **SPX-TPA** and **SPX-BT** in DCM with 0.1 M tetrabutylammonium hexafluorophosphate (TBAPF_6) as supporting electrolyte.

(a)



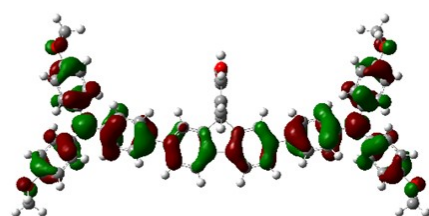
SPX-TPA

(b)



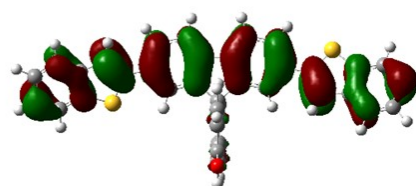
SPX-BT

(c)



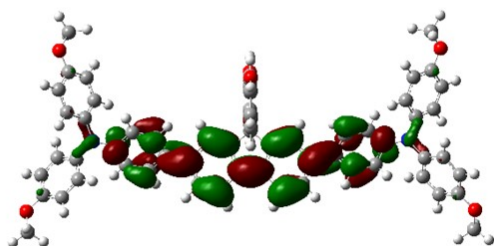
HOMO (-4.489 eV)

(d)



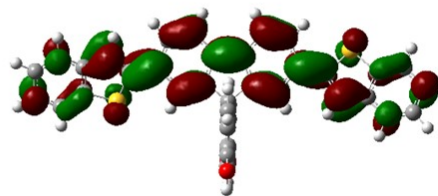
HOMO (-5.307 eV)

(e)



LUMO (-1.105 eV)

(f)



LUMO (-1.720 eV)

Fig. S2 (a and b) Optimized structure, (c and d) HOMO and (e and f) LUMO energy levels of SPX-TPA and SPX-BT.

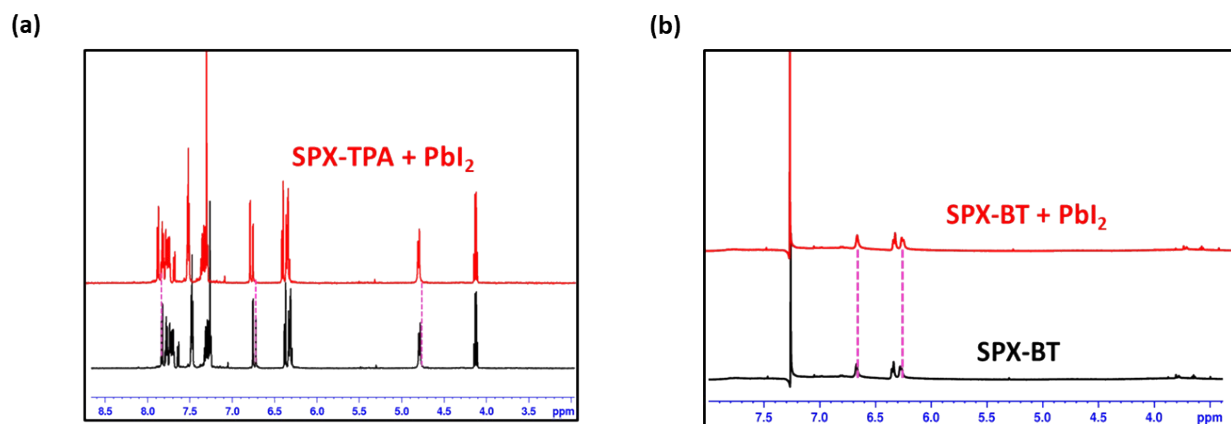


Fig. S3 NMR studies show the resonance signals of **SPX-TPA** (a) and **SPX-BT** (b) and their chemical interaction with PbI₂.

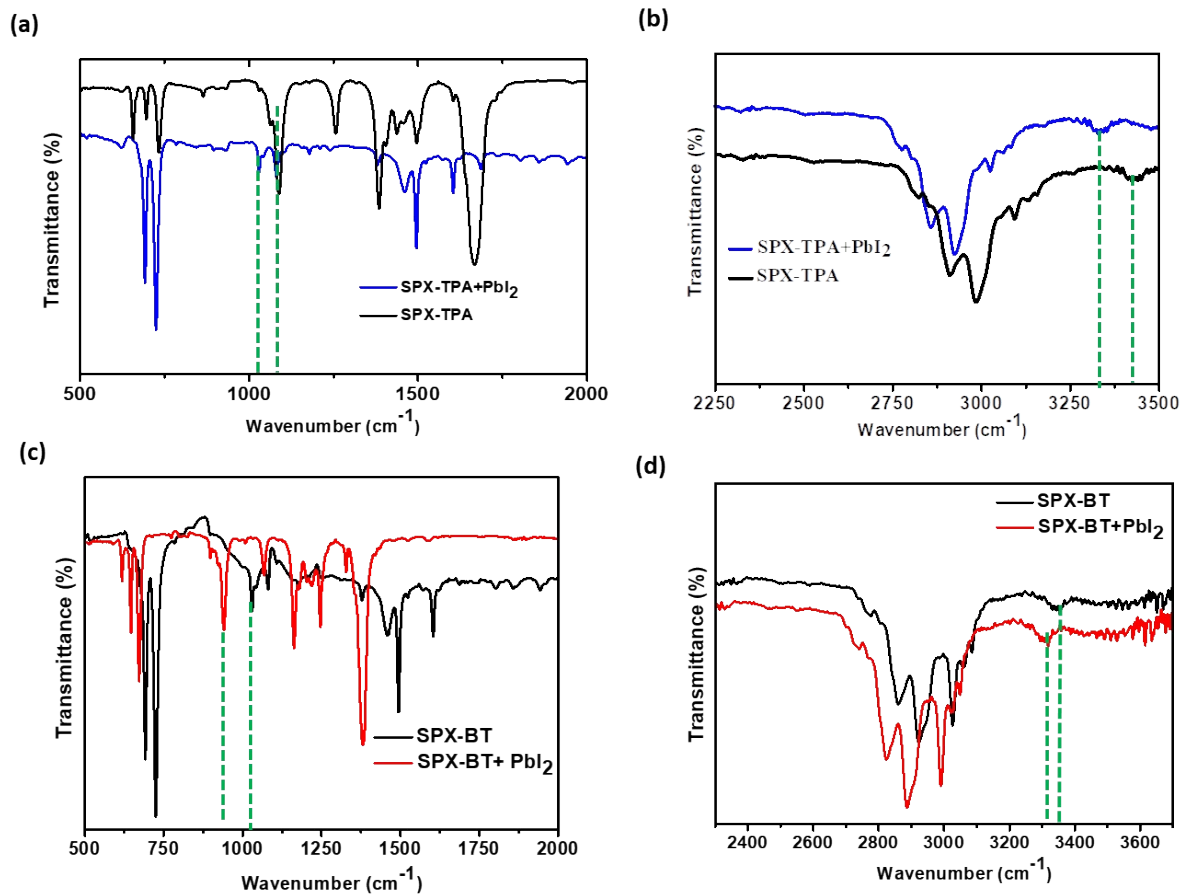


Fig. S4 FTIR spectra of SPX-TPA (a-b) and SPX-BT (c-d) treated with PbI₂.

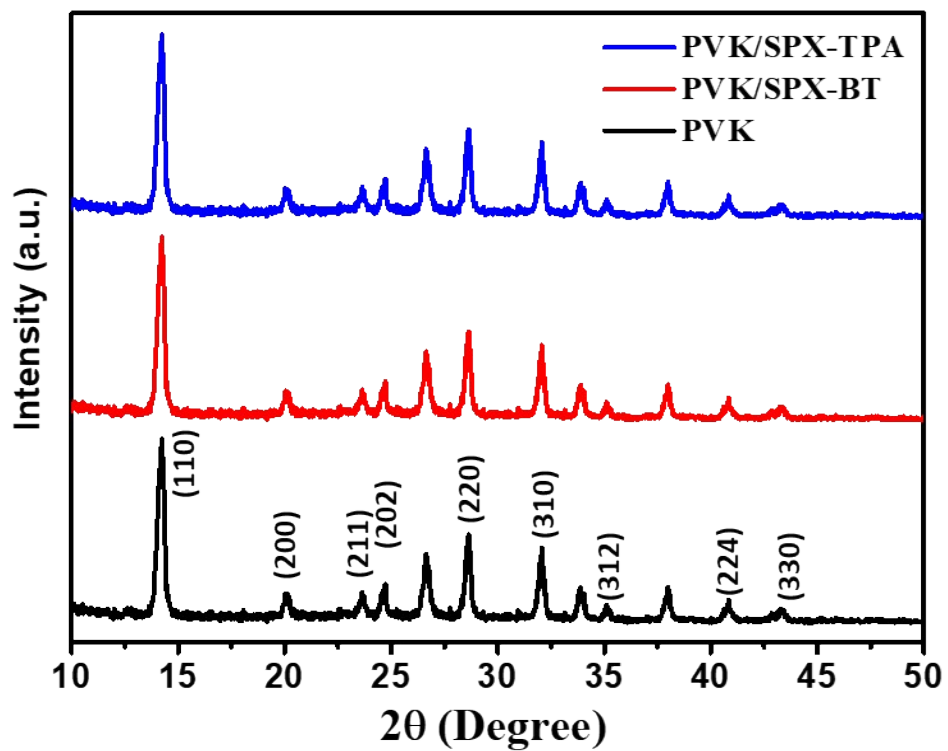


Fig. S5 XRD spectra of control PVK, PVK/SPX-TPA and PVK/SPX-BT.

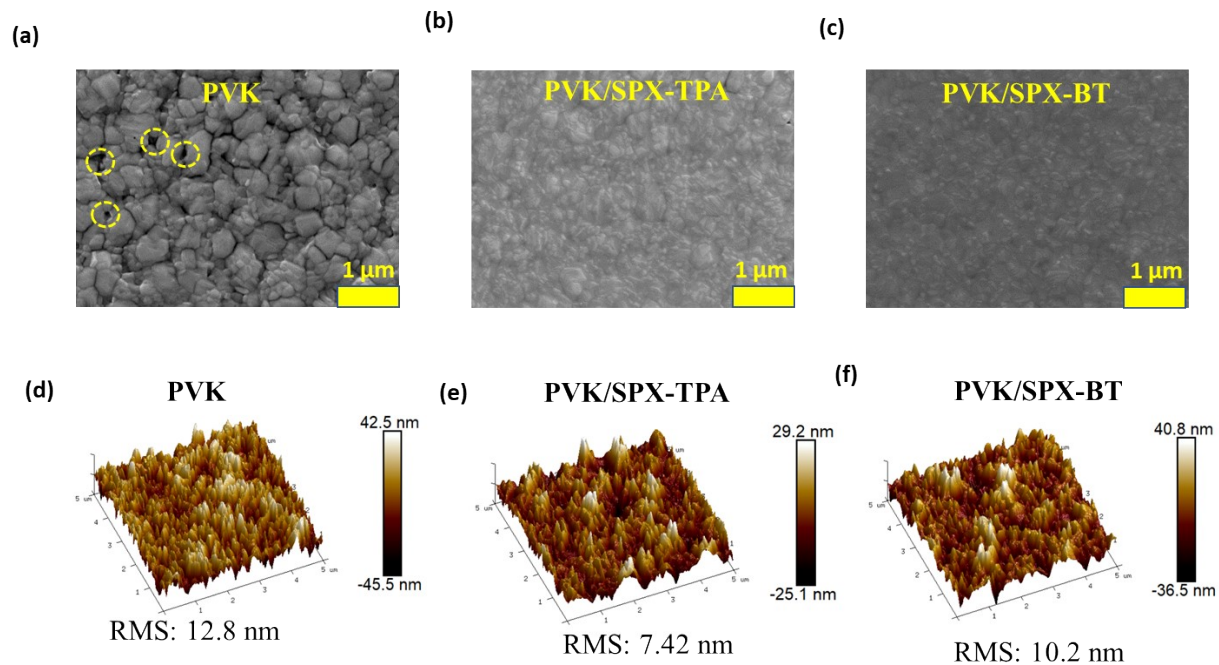


Fig. S6 Top-view SEM images (a) pristine PVK, (b) PVK-treated with **SPX-TPA**, and (c) PVK-treated with **SPX-BT**. AFM images (d) Control PVK, (e) PVK modified with **SPX-TPA**, and (f) PVK modified with **SPX-BT**.

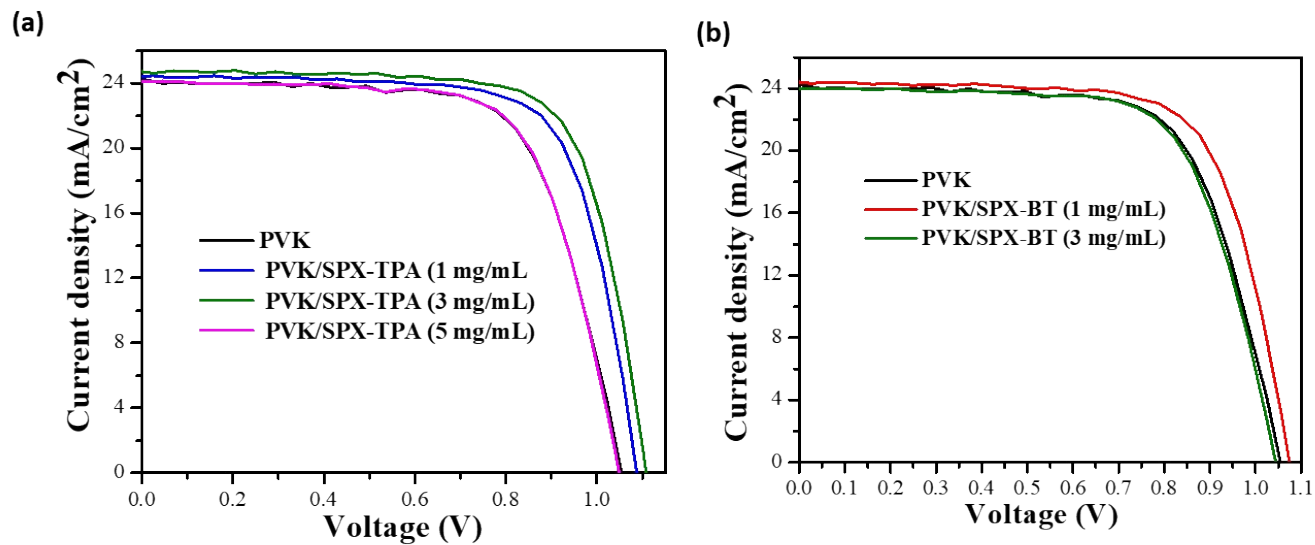


Fig. S7 J-V characteristics of MAPbI_3 -based PSCs fabricated with different concentrations of SPX-TPA (a) and SPX-BT (b).

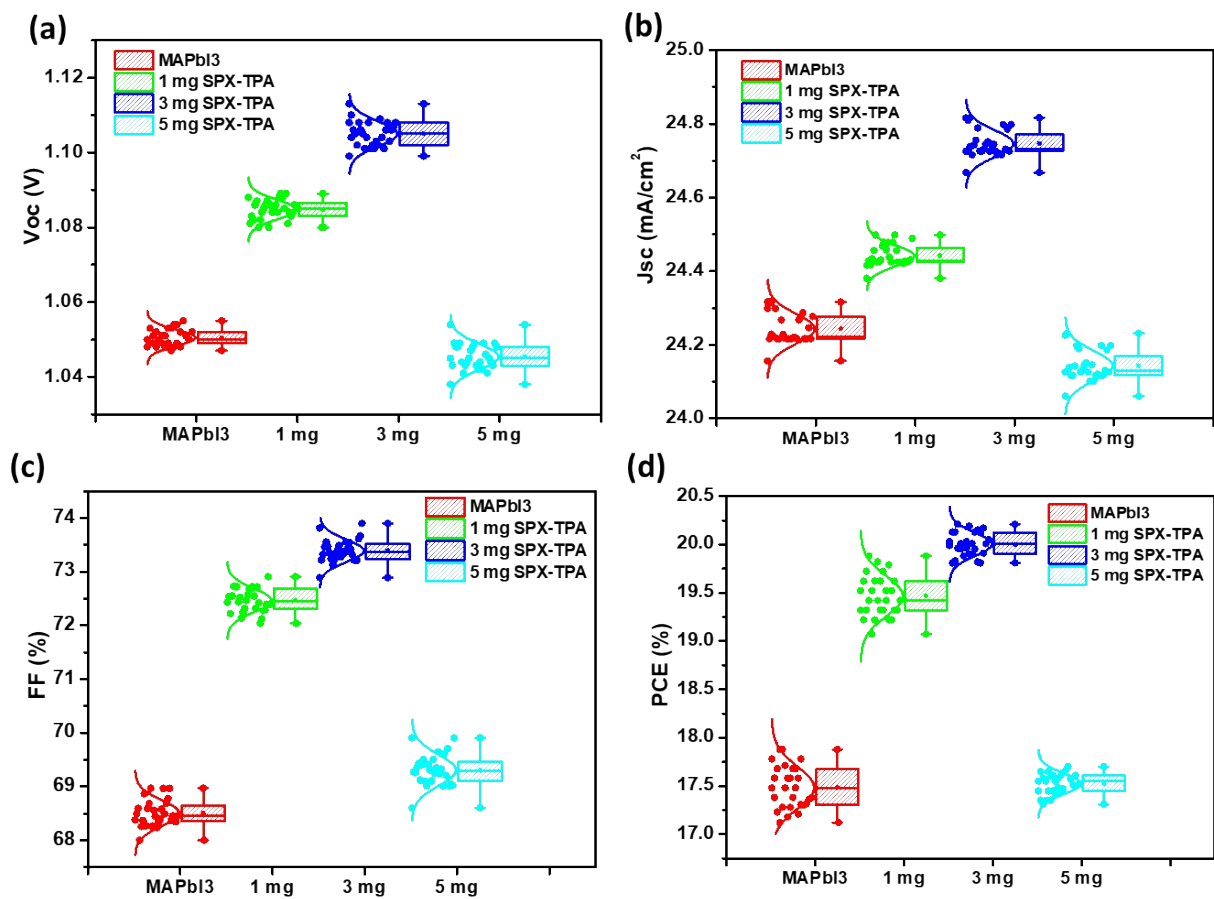


Fig. S8 The statistical distribution of (a) V_{oc} , (b) J_{sc} , (c) FF and (d) PCE of control PVK and PVK/SPX-TPA (28 cells) fabricated under the same conditions.

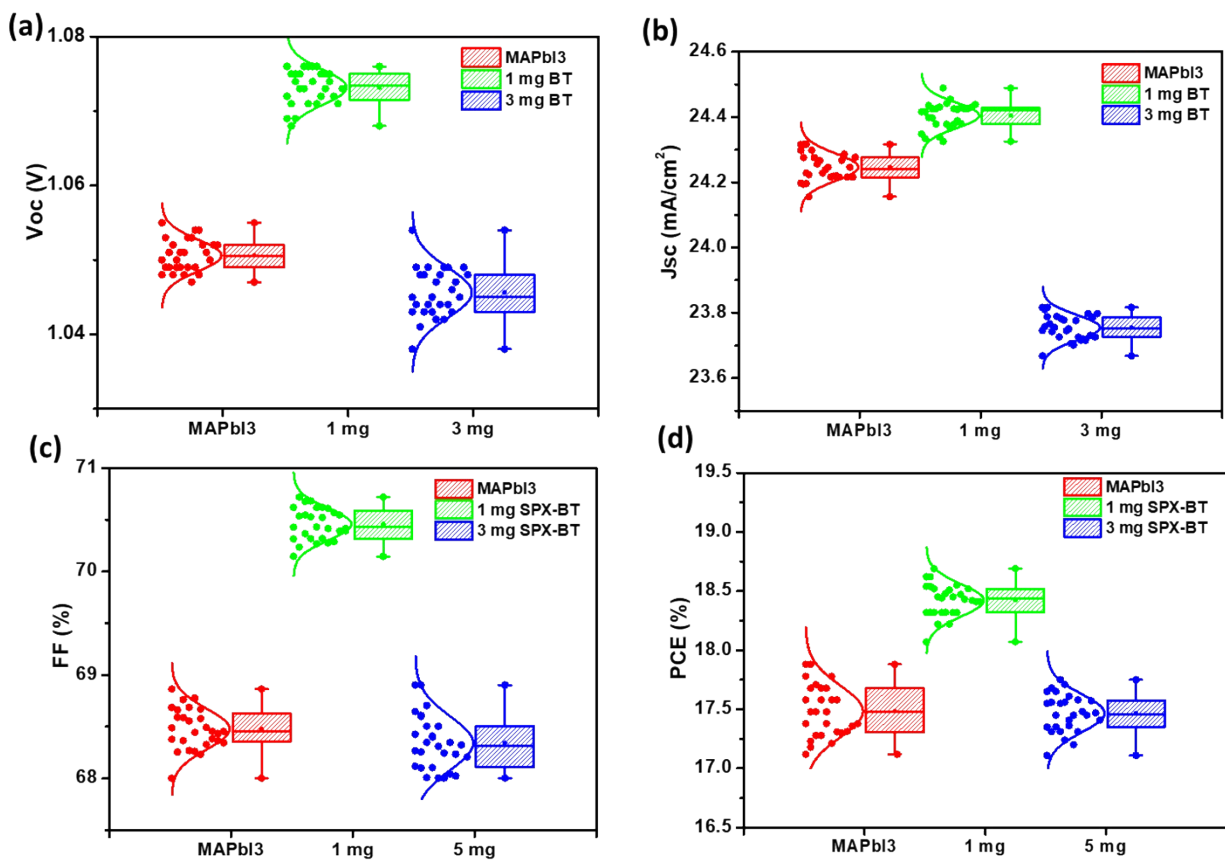


Fig. S9 The statistical distribution of (a) Voc, (b) Jsc, (c) FF and (d) PCE of PVK and PVK/SPX-BT (28 cells) fabricated under the same conditions.

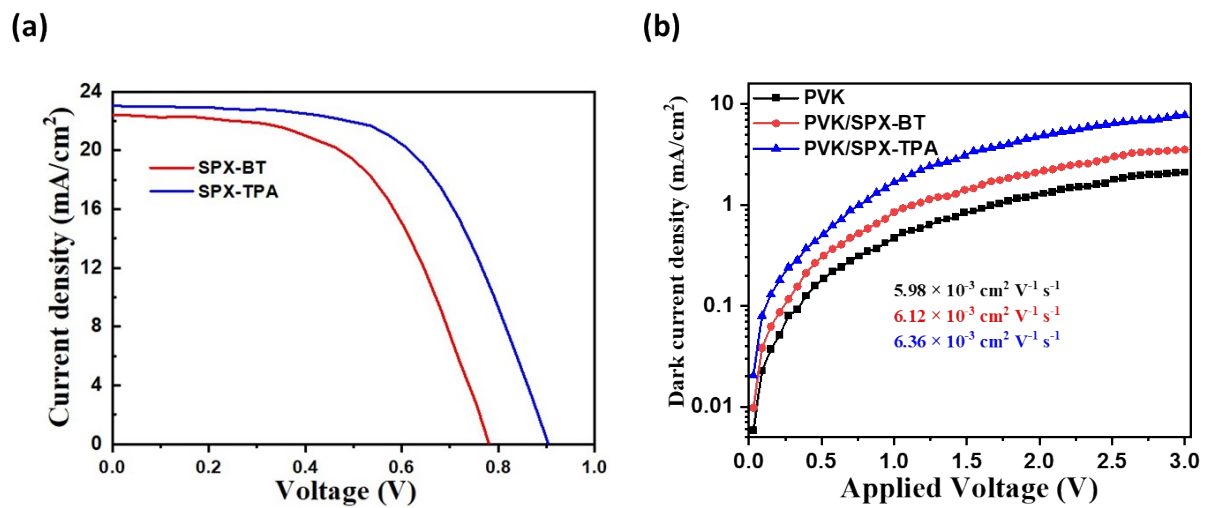


Fig. S10. (a) J - V characteristics of **SPX-BT** and **SPX-TPA** as HTMs. (b) The J - V characteristics of hole-only unipolar devices (ITO/PEDOT:PSS/PVK/HTIL /Spiro-OMeTAD/Au) under dark conditions.

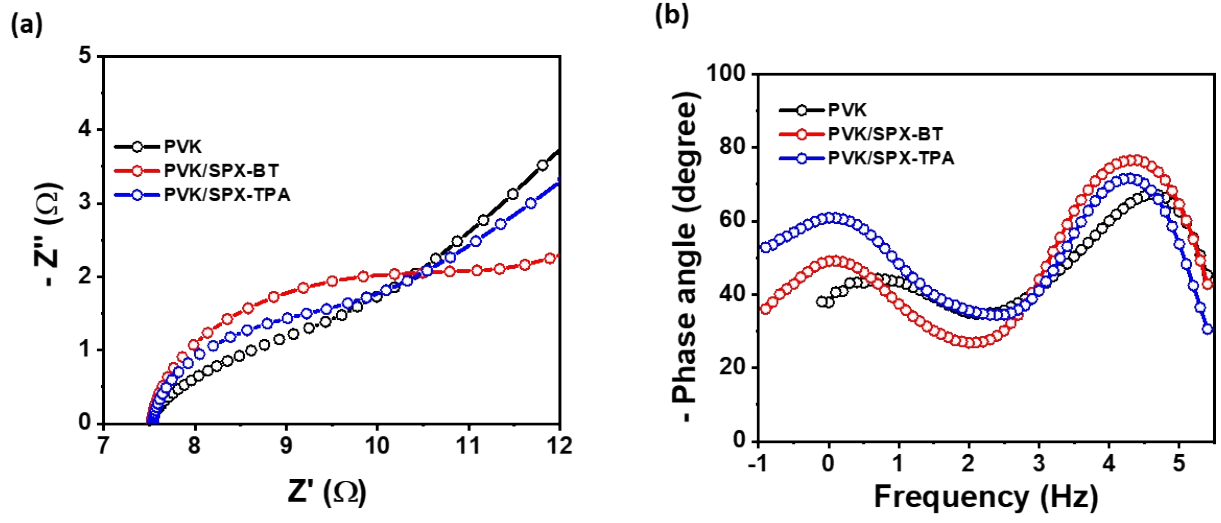


Fig. S11 (a) Enlarged view of Nyquist plot at high frequency. (b) Bode phase plots of control PVK, PVK/BT and PVK/TPA.

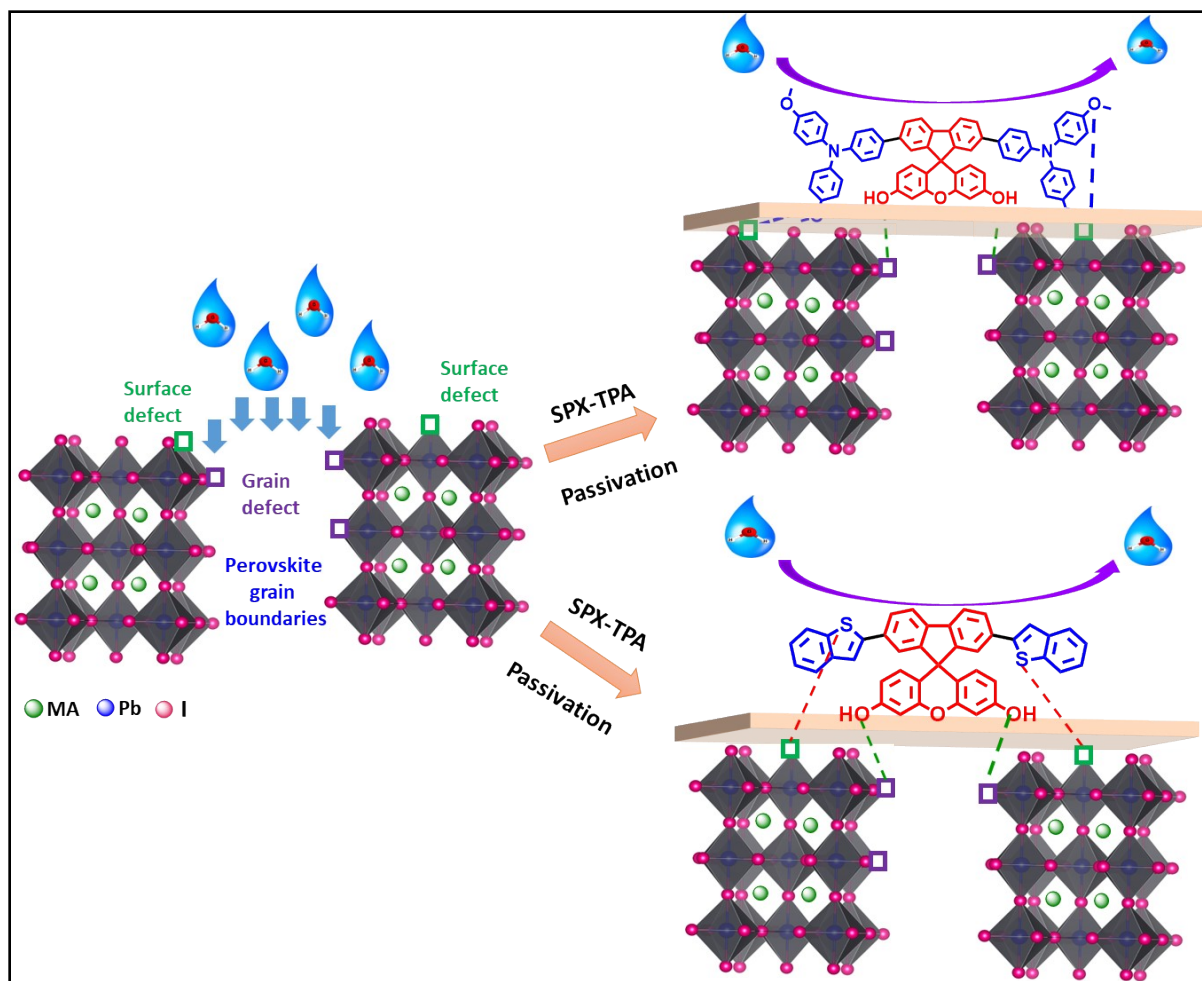


Fig. S12 Schematic representation of perovskite grain defects H₂O penetration and water repelling behavior of SPX-TPA and SPX-BT coated perovskite devices.



Fig. S13. Water contact angle measurement of (a) control PVK, (b) PVK/SPX-BT, and (c) PVK/SPX-TPA.

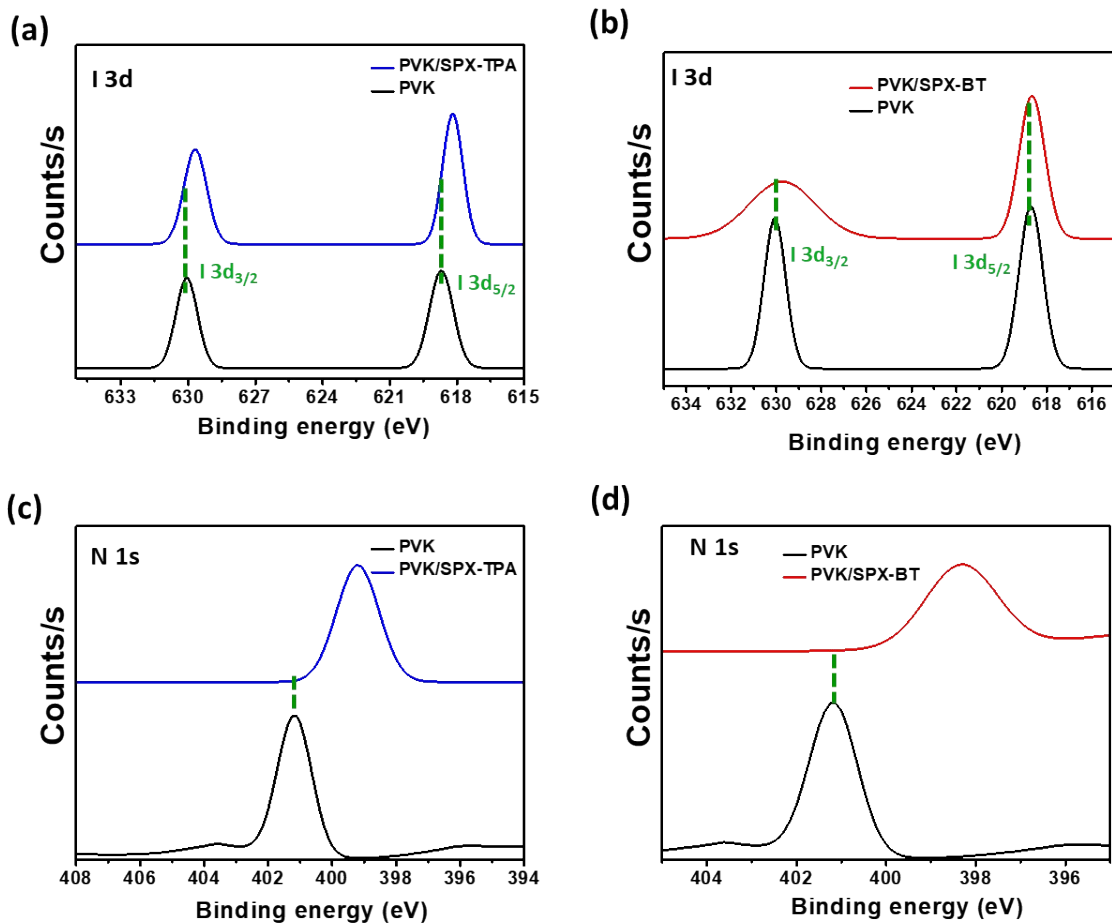


Fig. S14 (a) and (b) XPS spectra of I 3d and (c) and (d) N 1s for control PVK, PVK/SPX-TPA, and PVK/SPX-BT

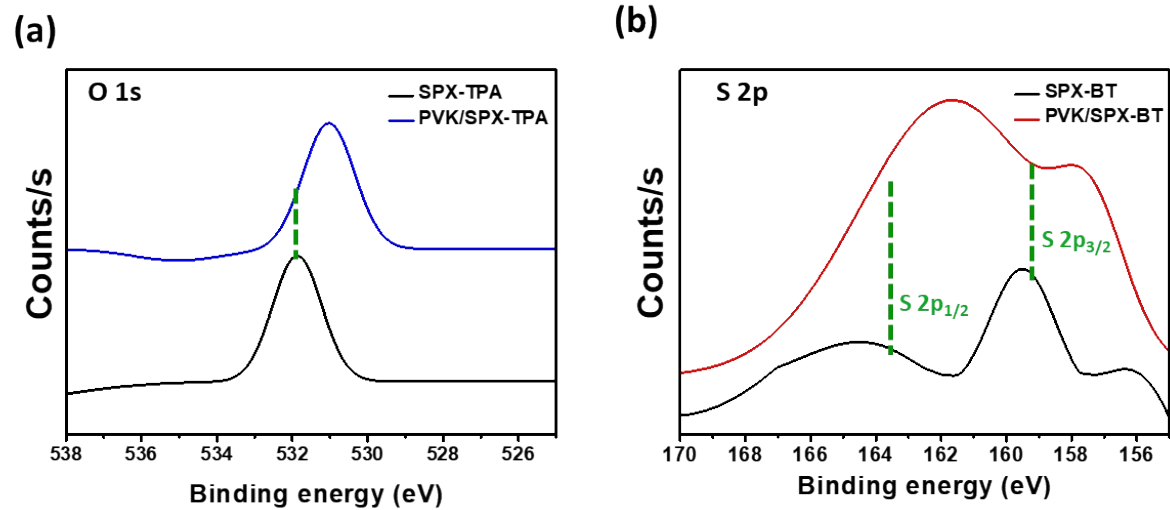


Fig. S15 (a) XPS spectra of O 1s and (b) S 2p for **SPX-TPA**, **SPX-BT**, **PVK/SPX-TPA** and **PVK/SPX-BT**.

Table S1. Optoelectronic properties of **SPX-TPA** and **SPX-BT**

Materials	λ_{max} (nm)	λ_{onset} (nm)	$E_{\text{o-o}}^{\text{Optical}}$	E_{ox} (eV)	HOMO (eV)	LUMO (eV)
SPX-TPA	383	420	2.95	0.58	-5.38	-2.43
SPX-BT	365	398	3.11	0.54	-5.34	-2.23

Table S2. TRPL data of Control PVK, PVK/SPX-BT, and PVK/SPX-TPA.

Device	τ_1	A_1	τ_2	A_2
PVK/Spiro	12.81	1262.90	47.03	346.40
PVK/SPX-BT/Spiro	4.68	895.64	38.23	56.30
PVK/SPX-TPA/Spiro	3.86	309.66	36.13	28.197

Table S3. Summarized PV performance of PSCs constructed with different concentrations of **SPX-TPA** and **SXP-BT**.

Device	V_{oc} (V)	J_{sc} (mA/cm ²)	FF (%)	PCE (%)	R_s	R_{sh}
PVK	1.054	24.21	68.26	17.77	37.63	9570.18
SPX-TPA (1 mg)	1.088	24.42	72.72	19.32	37.35	11295.61
SPX-TPA (3 mg)	1.108	24.72	73.11	20.03	33.32	10600.1
SPX-TPA (5 mg)	1.049	24.11	69.01	17.45	43.71	8067.53
SPX-BT (1 mg)	1.074	24.42	70.57	18.51	39.41	12020.07
SPX-BT (3 mg)	1.044	23.99	68.80	17.58	44.45	15643.03

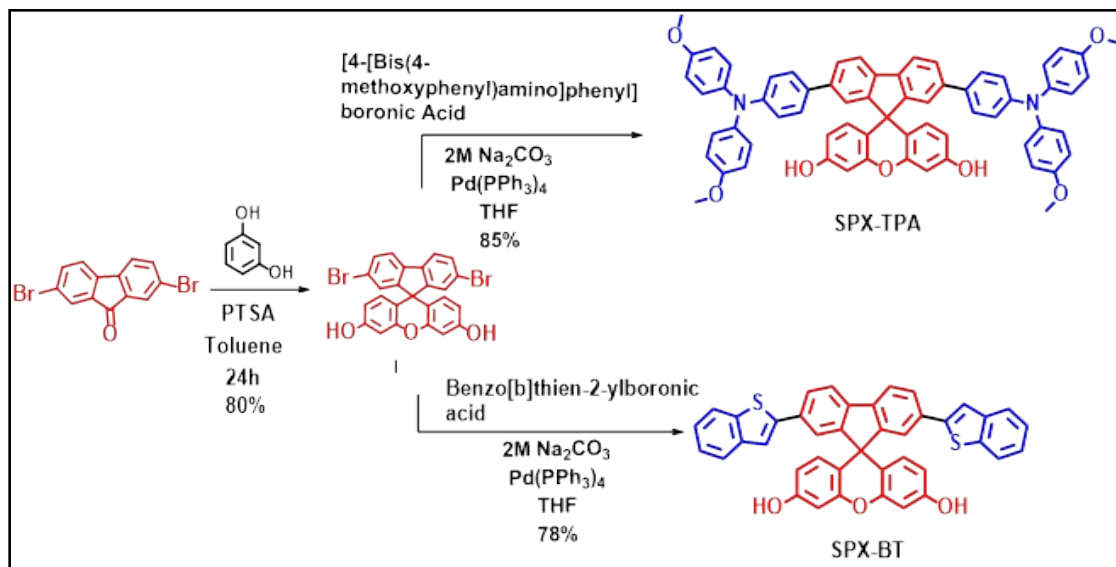
Table S4. Photovoltaic performance of **SPX-TPA** and **SPX-BT** as hole transporting materials.

Device	V_{oc} (V)	J_{sc} (mA/cm²)	FF (%)	PCE (%)
SPX-TPA	0.904	23.06	59.07	12.31
SPX-BT	0.781	22.40	55.86	9.78

Table S5. Interfacial charge transport parameters of PVK, PVK/BT and PVK/TPA devices

Device	R_s (Ω)	R_{ct} (Ω)	R_{rec} (Ω)	C_μ (μF)	τ_e (s)	$\chi^2 \times 10^{-3}$
PVK	7.62	4.97	32.99	5.835	0.03	6.71
PVK/SPX-BT	7.78	4.64	157.18	6.786	0.12	4.33
PVK/SPX-TPA	7.44	3.91	271.72	6.992	0.14	3.38

Synthesis



Scheme S1. Synthesis route of **SPX-TPA** and **SPX-BT**.

2,7-dibromospiro[fluorene-9,9'-xanthene]-3',6'-diol (**I**)

The synthesis of intermediate **I** have followed the previously reported literature.¹ To a 50 ml round bottom flask was charged with 2, 7-Dibromo-9-fluorenone (500 mg, 1.479 mmol), resorcinol (814.26 mg, 7.395 mmol), p-TsOH (50 mg, 0.295 mmol), and toluene (25 mL). Then reflux the mixture upto 12h, and cool to room temperature. After that 100 mL of water was added to the reaction mixture and continued the reaction further 0.5 h at room temperature. The yellow color precipitated from the reaction mixture which was isolated by the filtration process. Further, the crude product was dissolved in alcohol (100 mL) and filtrated. Finally, the solution was concentrated by vacuum evaporation and purified by column chromatography using silica gel, petroleum ether/EtOAc (3:1), and afford required product-I as a brown solid (yield 80%). ¹H NMR (400 MHz, CDCl₃): δ (ppm) 7.60 (d, J = 8.1 Hz, 2H), 7.46 (dd, J = 8.1, 1.8 Hz, 2H), 7.25 – 7.18 (m, 2H), 6.68 (d, J = 2.5 Hz, 2H), 6.32 (dd, J = 8.6, 2.6 Hz, 2H), 6.21 (d, J = 8.6 Hz, 2H), 5.09 (s, 2H). ¹³C NMR (101 MHz, CDCl₃) δ 156.94, 155.80, 137.62, 131.16, 128.90, 122.42, 121.36,

115.60, 115.43, 111.63, 103.39, 29.74. ESI-MS calcd for $C_{25}H_{14}Br_2O_3$ $[M+H]^+$ m/z 522.03; found 523.01.

3,6-bis(4-(bis(4-methoxyphenyl)amino)phenyl)spiro[fluorene-9,9'-xanthene]-3',6'-diol (SPX-TPA)

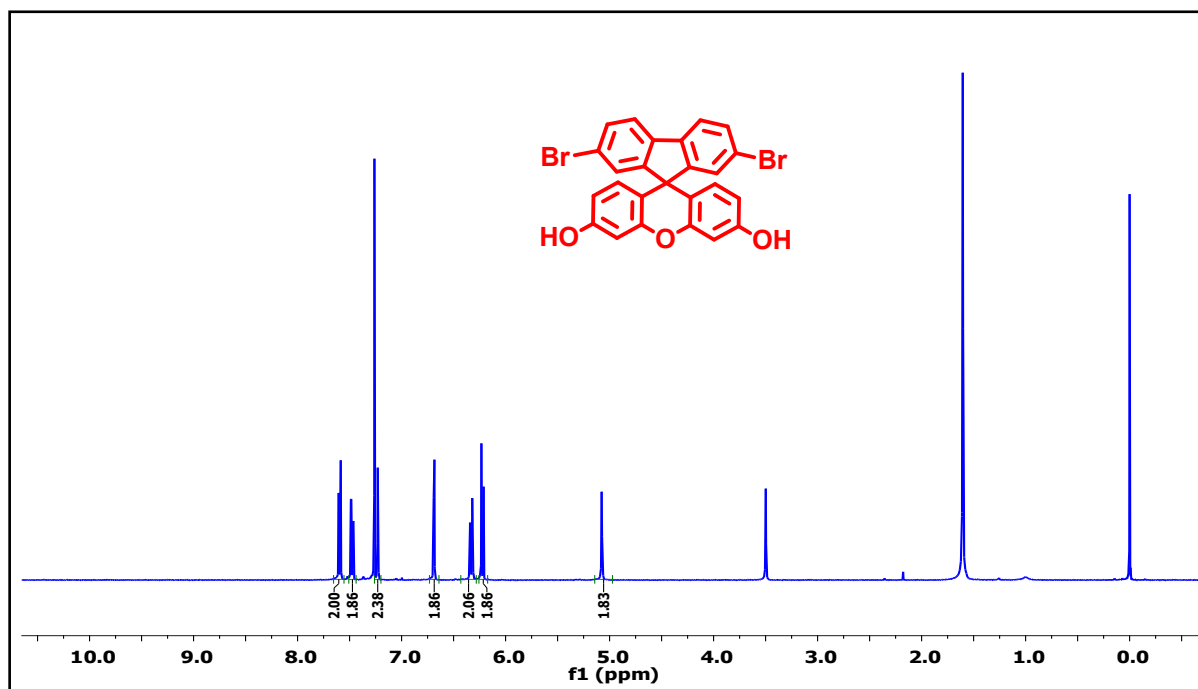
A round bottom flask (50 mL) was charged with intermediate I (100 mg, 0.191 mmol), [4-[Bis(4-methoxyphenyl)amino]phenyl]boronic Acid (140 mg, 0.402 mmol), 2M sodium carbonate (2M Na_2CO_3) (1.06 g) and tetrahydrofuran (THF) (20 mL) in an inert gas atmosphere condition. Before going to the addition of tetrakis (triphenyl phosphine) palladium (0) ($Pd(PPh_3)_4$) (10%), degassed the reaction mixture up to 30 minutes, then the reaction was refluxed upto 12 h at 70 °C. The completion of the reaction was confirmed by TLC, and then the reaction solvent was removed by rotary evaporation. The crude product was worked with water and brine (NaCl) solution and finally concentrated with the rotary evaporation process. The final crude material was purified by column chromatography technique using silica gel with DCM and hexane to yield of **SPX-TPA** as a green color solid (85% yield). 1H NMR (500.1 MHz, $CDCl_3$): δ 8.75-8.50 (s, 4H), 7.80-7.70 m, 2H), 7.61-7.50 (m, 2H), 7.42-7.7.21 (m, 6H), 7.10-6.85 (m, 6H), 6.91 (d, 4H), 6.84-6.75 (m, 7 H), 6.50-6.31 (m, 5H), 5.12-5.10 (m, 2H), 3.84 (s, 12H). ^{13}C (75.4 MHz, $CDCl_3$): δ 158.18, 157.96, 155.91, 155.56, 152.03, 149.70, 148.19, 146.56, 141.44, 140.80, 137.75, 132.69, 132.39, 131.12, 128.80, 126.54, 123.54, 120.14, 117.01, 114.72, 111.37, 111. 19, 102.43, 67.80, 55.74. LC-MS: calcd. for $C_{65}H_{50}N_2O_7$, $[M]^+$ m/z 971.02; found: 971.12, CHNS: $C_{65}H_{50}N_2O_7$ calcd, C 80.39, H 5.19, N 2.88, O 11.53; found C 80.45, H 5.21, N 2.91, O 11.51.

3,6-bis(benzo[b]thiophen-2-yl)spiro[fluorene-9,9'-xanthene]-3',6'-diol (SPX-BT)

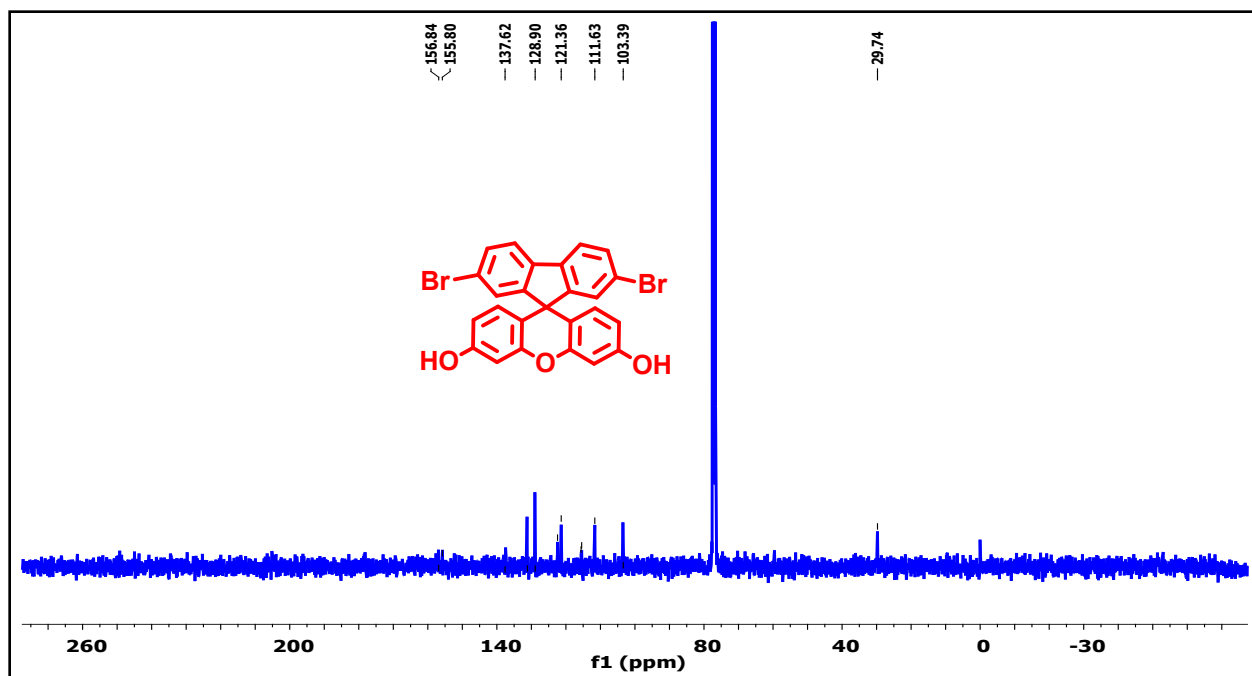
To a round bottom flask (50 mL) was charged with intermediate I (200 mg, 0.381 mmol), benzo[b]thiophene-2-boronic acid (203 mg, 1.140 mmol), 2M Na_2CO_3) (1.06 g) and tetrahydrofuran (THF) (30 mL) in an inert gas atmosphere condition. Before going to the addition of $Pd(PPh_3)_4$ catalyst (10%), degassed the reaction mixture up to 30 minutes, and then the reaction was refluxed upto 12 h at 70 °C. The completion of the reaction was confirmed by TLC, and then and cool to room temperature. Further, THF solvent was removed by rotary evaporation, the

resultant solid product was worked with water and brine solution. The final crude solid material was subjected to column chromatography using silica gel with DCM and hexane as eluents to yield of **SPX-BT** as a brown color solid (78% yield). ^1H NMR (500.1 MHz, CDCl_3): δ 7.98-7.38 (m, 6H), 7.18-6.87 (m, 4H), 6.88-6.60 (m, 5H), 6.59-6.01 (m, 7H), 3.88-3.68 (m, 2H). The limited solubility of the compound precluded ^{13}C NMR characterization. LC-MS: calcd. for $\text{C}_{41}\text{H}_{24}\text{O}_3\text{S}_2$, $[\text{M}]^+ m/z$ 628.12; found: 628.10, CHNS: $\text{C}_{41}\text{H}_{24}\text{O}_3\text{S}_2$ calcd, C 78.32, H 3.85, O 7.63, S 10.20; found C 78.31, H 3.83, O 7.61, S 10.22.

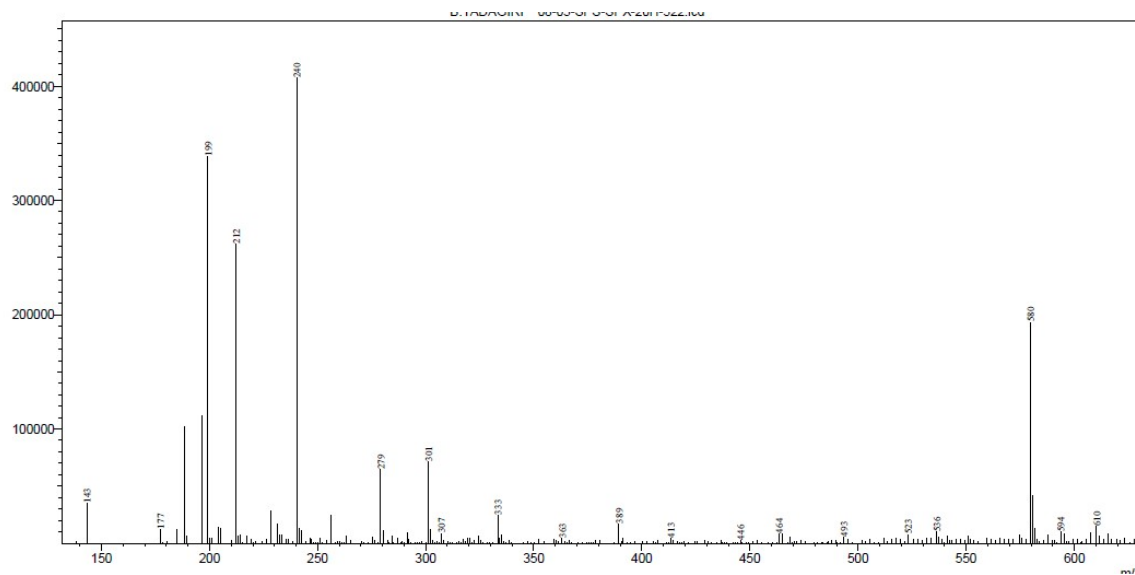
Copies of NMR Spectra



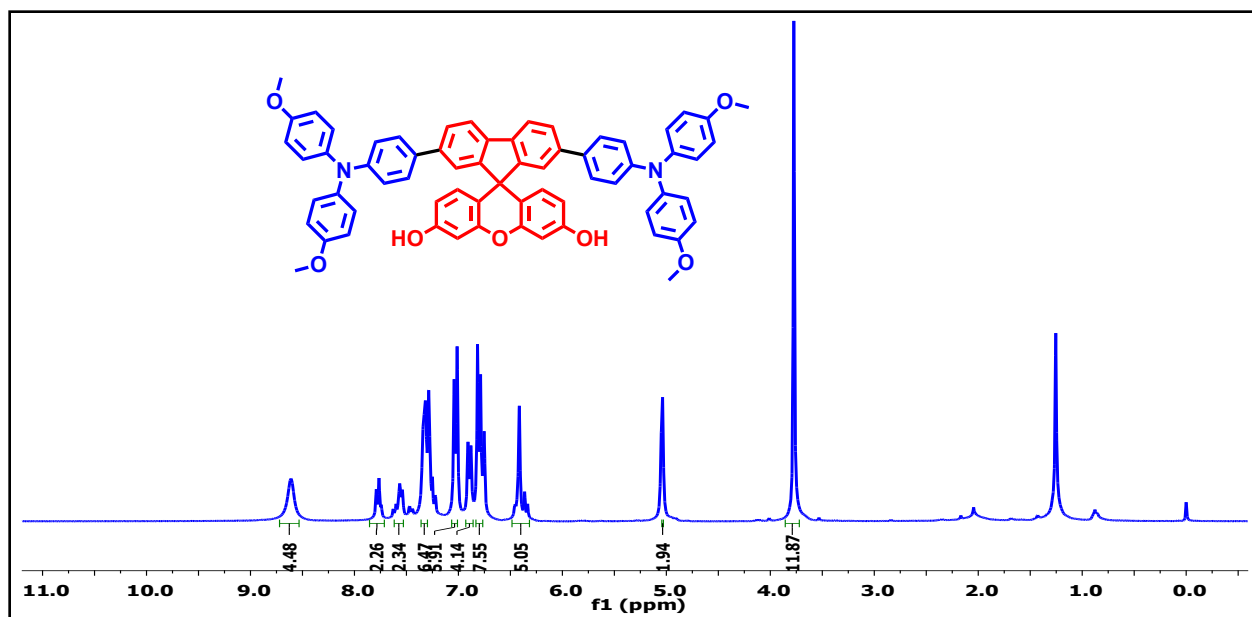
¹H-NMR spectra of intermediate I



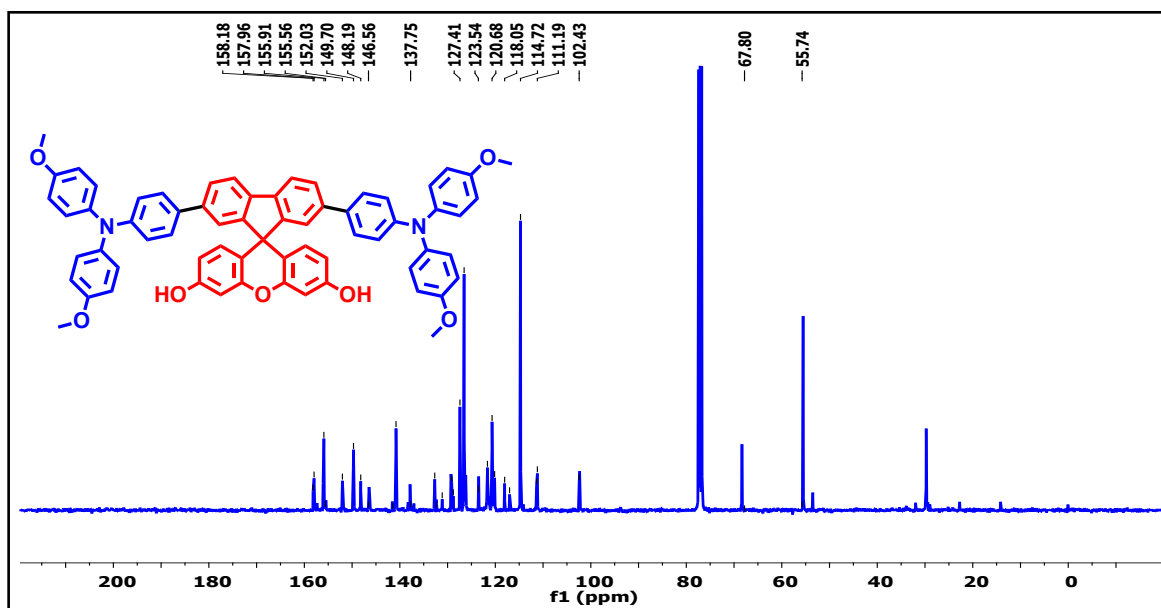
¹³C-NMR spectra of intermediate I



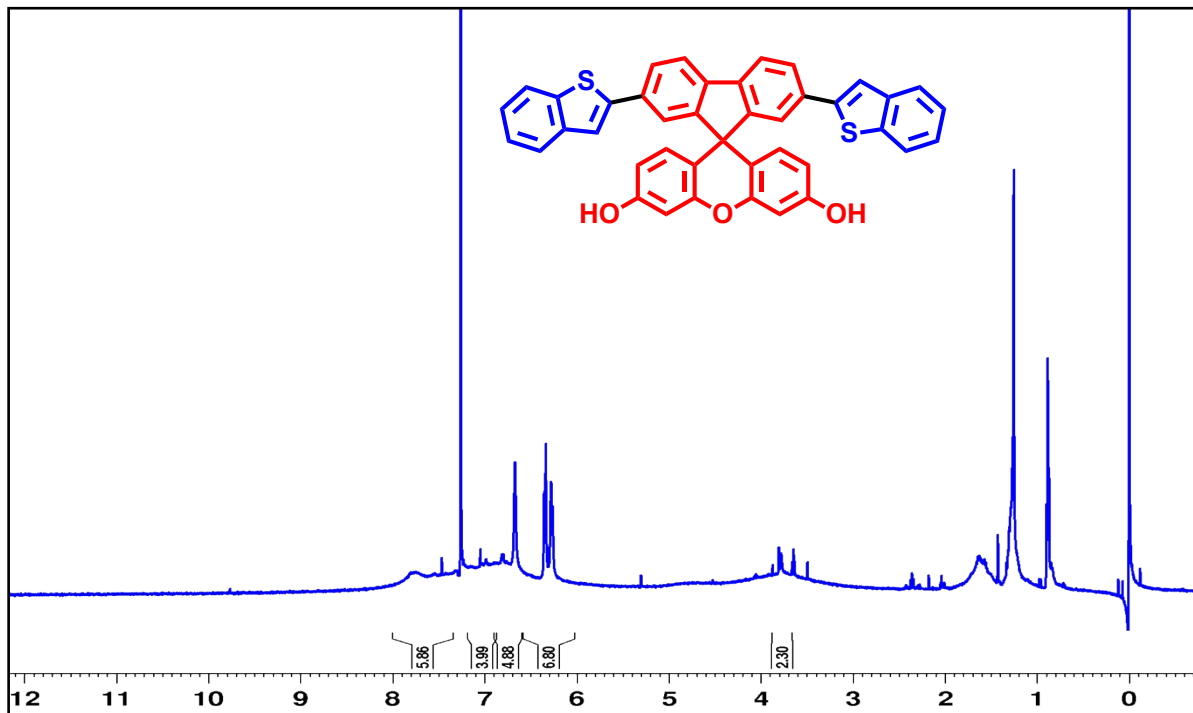
ESI mass spectra of compound I



¹H-NMR spectra of SPX-TPA



¹³C-NMR spectra of SPX-TPA



¹H-NMR spectra of **SPX-BT**

Reference

1. B. Yadagiri, T. H. Chowdhury, Y. He, R. Kaneko, A. Islam and S. P. Singh; *Mater. Chem. Front.*, 2021, **5**, 7276–7285.